Carbohydrate Polymers 86 (2011) 1266–1272

Contents lists available at ScienceDirect

Carbohydrate Polymers

journal homepage: www.elsevier.com/locate/carbpol

Characterization of polyelectrolytes complexes based on *N*,*N*,*N*-trimethyl chitosan/heparin prepared at different pH conditions

Alessandro F. Martins, Antonio G.B. Pereira, André R. Fajardo, Adley F. Rubira, Edvani C. Muniz*

Grupo de Materiais Poliméricos e Compósitos – GMPC, Departamento de Química, Universidade Estadual de Maringá – UEM, Av. Colombo 5790, CEP 87020-900 Maringá, Paraná, Brazil

ARTICLE INFO

Article history:
Received 26 February 2011
Received in revised form 7 June 2011
Accepted 9 June 2011
Available online 16 June 2011

Keywords:
Polyelectrolytes complexes
Chitosan
N,*N*,*N*-trimethyl chitosan
Heparin
Biopolymers

ABSTRACT

N,*N*,*N*-trimethyl chitosan (TMC) was synthesized through the *N*-methylation of chitosan (CHT) and characterized by FTIR and ^{1}H NMR spectroscopy. Polyelectrolyte complexes (PECs) based on TMC and heparin (HP) were prepared at different pHs (5, 8, 10 and 12) and characterized through FTIR spectroscopy, DSC and TGA curves and WAXS profiles. It was verified that the higher the pH of feed solution used for the PEC formation the higher is the thermal stability of PECs. Under basic conditions, the complexation between TMC and HP was more effective and alterations on WAXS profiles of PECs in relation to the precursor (TMC) were clearly observed. In addition, WAXS profiles show that the PEC crystallinity depends on the pH used for the complexation. These results are consistent with the FTIR, DSC, and TGA data. Due to the more intense electrostatic interactions, at higher pHs the unlike polymers chains (TMC and HP) are close enough to produce more stable PECs.

1. Introduction

Chitosan (CHT) is a linear polysaccharide obtained from deacetylation of chitin (Abdel-Fattah, Jiang, El-Bassyouni, & Laurencin, 2007; Chen et al., 2008; Chen, Mo, He, & Wang, 2008; Kweon, Song, & Park, 2003). Chitin is the second most abundant polysaccharide in the world (Liu et al., 2009). Due to biocompatibility and good mechanical properties of CHT, many papers focused on this polymer have been published in the scientific literature reporting its biomedical applications such as drug delivery systems (George & Abraham, 2006; Mi, Sung, Shyu, Su, & Peng, 2003; Yuan et al., 2007; Yuan, Hein, & Misra, 2010; Piai, Lopes, Fajardo, Rubira, & Muniz, 2010). In spite of many important properties that could result in CHT having a wide range of applications, the low solubility in water at both neutral and basic conditions restrict the application of CHT-based materials (Sadeghi et al., 2008; Thanou, Verhoef, & Junginger, 2001). However, chemical modifications of CHT can overcome such limitation as well as give properties compared with native CHT (Chen, Zhang, et al., 2008; Chen, Mo, et al., 2008; Jintapattanakit et al., 2007).

A good example of CHT-modified polymer with improved properties compared to CHT is the *N*,*N*,*N*-trimethyl chitosan (TMC). The TMC is obtained from the *N*-methylation of CHT (Le Dung, Milas, Rinaudo, & Desbriires, 1994; Sieval et al., 1998). This polymer possesses linear chains and permanently charged sites due to the partially quaternized nitrogen atoms. In the last years, materials based on TMC have evoked great interest since that TMC, sometimes, presents better properties than those found in CHT (Mourya & Inamdar, 2009; Van der Merwe, Verhoef, & Verheijden, 2007). For instance, CHT-common properties such as mucoadhesion, nontoxicity and biodegradability remain in TMC (Li et al., 2010; Mourya & Inamdar, 2009; Van der Merwe et al., 2007). In addition, *in vitro* (Caco-2 cells) and *in vivo* (rat and pork) studies proved that TMC increases the permeation of hydrophilic compounds (peptides, and some proteins) in relation to CHT (Kotzé et al., 1997; Sayin et al., 2008; Snyman, Hamman, Kotze, Rollings, & Kotzé, 2002; Thanou, Florea, Langemeyer, Verhoef, & Junginger, 2000). In addition, the antibacterial power of TMC is ca. 100–500 fold more intense than CHT (Xu, Xin, Li Mingchun, Huang, & Zhou, 2010). It is worth mentioning that TMC is soluble at wide range of pH and therefore overcomes the limitations in solubility presented by CHT at neutral and basic conditions. For these reasons, it sounds reasonable to predict that TMC is very promising in the pharmaceutical and medical fields (Chang, Xiao, & Du, 2009; Thanou, Florea, et al., 2000).

The chemical structure of TMC is an important feature, which determines the physical and chemical properties of this polymer. Researchers have shown that the amount of methyl groups inserted on amino groups from TMC influences many properties of TMC like its thermal stability, for instance (Polnok, Borchard, Verhoef, Sarisuta, & Junginger, 2004; Britto & Campana-Filho, 2004). The percentage of $-N^+(CH_3)_3$ and $-N(CH_3)_2$ groups on the structure of

* Corresponding author. Tel.: +55 44 3011 3664; fax: +55 44 3011 4215.
E-mail addresses: ecmuniz@uem.br, curtimuniz@gmail.com (E.C. Muniz).

0144-8617/$ – see front matter © 2011 Elsevier Ltd. All rights reserved.
doi:10.1016/j.carbpol.2011.06.024

TMC is defined by the degree of quaternization (DQ) and the degree of disubstitution (DD) parameters (Hamman and Kotzé, 2001).

Heparin (HP) is a biopolymer of linear chains that presents many applications in medical and pharmaceutical areas (Lin et al., 2009; Zhu, Ming, & Jian, 2005; Oyarzun-Ampuero, Brea, Loza, Torres, & Alonso, 2009). It acts indirectly in the blood coagulation mechanism, stimulates cellular growth (Lin et al., 2009; Zhu et al., 2005; Oyarzun-Ampuero et al., 2009) and has antibacterial effects (Fu, Ji, Yuan, & Shen, 2005). HP is an anionic polysaccharide that, at specific conditions, could be used to form polyelectrolytes complexes (PECs) with cationic polymers (Kweon et al., 2003).

The objective of this work was the synthesis and physical and chemical characterization of TMC, the preparation of polyelectrolyte complexes (PECs) based on TMC/HP in a wide range of pH and evaluation of several physical and chemistry properties of the so-obtained PECs. These targets are justified by the excellent properties of TMC and HP, and it is expected that such PECs have potential useful opportunities in the biomaterial field.

2. Experimental

2.1. Materials

Chitosan (CHT, CAS 9012-76-4) with deacetylation degree equal to 85% and average molecular weight 87×10^3 g mol^{-1} was purchased from Golden-Shell Biochemical (China); Methyl iodide (CAS 74-88-4) and *N*-methyl-2-pyrrolidinone (NMP, CAS 872-50-4) were both purchased from Sigma. Kin Master (Brazil) kindly supplied heparin sodium salt (HP, CAS 9041-08-1). Other reactants such as sodium hydroxide, sodium iodide, sodium chloride, hydrochloric acid, ethanol, and diethyl ether were also utilized in this work. All reactants were used as received without further purification.

2.2. Methods

2.2.1. Synthesis of TMC

The methodology employed for the synthesis of TMC was adapted from previously reported procedures (Le Dung et al., 1994; Sieval et al., 1998). In this method, TMC is synthesized via a reductive methylation of chitosan utilizing methyl iodide (CH_3I) in presence of a strong base (NaOH), at 60 °C. CHT and sodium iodide (NaI) were dissolved in NMP in a water bath at 60 °C with magnetic stirring. After, NaOH aqueous solution (15 wt.%/vol.%) and CH_3I were added in the resultant solution. The system was kept stirring for a while and the product was collected after precipitation utilizing ethanol. Therefore, the precipitate was separated by centrifugation process, washed several times with ethanol and diethyl ether portions, filtered, and dried under vacuum.

The product obtained in the first step was the *N*,*N*,*N*-trimethyl chitosan iodide (Thanou, Verhoef, Marbach, & Junginger, 2000). As a second step, this product was dissolved in NMP under a water bath at 60 °C and magnetic stirring. Again, after the complete solubilization, ca. 20 min, NaOH aqueous solution (15 wt.%/vol.%) and CH_3I was added in the resultant solution. After this time, the product was collected and dried according to procedures described above. In a final step, the resultant product was solubilized in sodium chloride (NaCl) aqueous solution (10 wt.%/vol.%) for exchanging the iodide ion (I^-) by chloride ion (Cl^-). The synthesized product was characterized by FTIR spectroscopy.

2.2.2. Preparation of polyelectrolytes complexes (PECs) of TMC and HP

The influence of the pH of feed solution during the complexation of TMC and HP on some PEC properties was investigated. The PECs were formed at different pH conditions while the volume-ratio TMC-solution to HP-solution was kept constant. The following procedure was used: aqueous solution of TMC (0.4 g of TMC in 40 ml of distilled water) was prepared. The TMC-solution was split in four aliquots of 10 ml. The pH of each aliquot was adjusted to a desired value (5, 8, 10 and 12) by adding aqueous solution of HCl or NaOH. Afterwards, 3 ml of a previously prepared HP-solution (1 wt.%/vol.%), at desired pH (5, 8, 10 and 12) was slowly dropped into a respective TMC-solution aliquot, at room temperature and under magnetic stirring (Martins, Piai, Schüquel, Rubira, & Muniz, 2011). The notation PEC5, PEC8, PEC10 and PEC12 were used for correlating the PEC to pH of preparation. After the PECs formation, the samples were frozen in liquid nitrogen and lyophilized (Christ Gefriertrocknungsanlagen) at −55 °C for 24 h. After drying the PECs were characterized through FTIR spectroscopy, thermal analysis and wide angle X-ray scattering (WAXS).

2.2.3. FTIR spectroscopy

FTIR was used to characterize the raw materials (CHT and HP) and the new materials prepared (TMC and PECs). In each case, KBr pellets at 1 wt.% were prepared. The equipment from Shimadzu Scientific Instruments (Model 8300, Japan) was used at the following conditions: range of 4000–500 cm^{-1}, resolution of 4 cm^{-1} obtained by cumulating 64 scans.

2.2.4. Thermal analysis through DSC and TGA

DSC runs of PECs were performed on a calorimeter (Netzsch, model STA 409 PG/4/G Luxx, USA) operating at the following conditions: heating rate of 10 °C min^{-1}, nitrogen flow rate of 50 ml min^{-1}, temperature range from 25 to 400 °C. TGA analysis of PECs were carried out on a thermogravimetric analyzer (Netzsch, model STA 409 PG/4/G Luxx, USA) at a rate of 10 °C min^{-1} under nitrogen atmosphere with flow rate of 50 ml min^{-1}, temperature range from 25 to 600 °C.

2.2.5. WAXS profiles

WAXS profiles of raw materials (CHT and HP) and of synthesized ones (TMC and PECs of TMC/HP) were recorded on a diffractometer Shimadzu (model XRD-600, Japan) equipped with a Ni-filtered Cu-K_α radiation. The WAXS profiles were collected in a scattering range (2θ) from 5° to 70°, with resolution of 0.02°, at a scanning speed of 2° min^{-1}. The analyses were performed by applying an accelerating voltage of 40 kV and a current intensity of 30 mA.

3. Results and discussion

3.1. Characterization of TMC

The limited solubility hinders the use of CHT and CHT-based materials to be applied on environments with alkaline conditions like the small intestine, for instance (Chang et al., 2009; Thanou, Florea, et al., 2000). The reductive methylation of CHT for obtaining TMC is a good strategy for overcoming such limitations because TMC is soluble in distilled water and in alkaline or acidic aqueous solutions and the good properties of CHT are present in TMC and, occasionally, some are improved.

The solubility of TMC at whole range of pH is due to the shifting in charge density originated by methylation of primary amino groups on CHT. The scheme for such reaction is shown in Fig. 1.

The FTIR spectra of raw CHT and of TMC are shown in Fig. 2. Some differences are clearly seen by comparison of both spectra. For instance, the band at 1484 cm^{-1} present on the TMC spectrum, assigned to angular deformation of C–H bonds of methyl groups (–CH_3), is not observed on CHT spectrum. Another evidence of CHT modification/TMC formation is the absence of band at 1601 cm^{-1} in

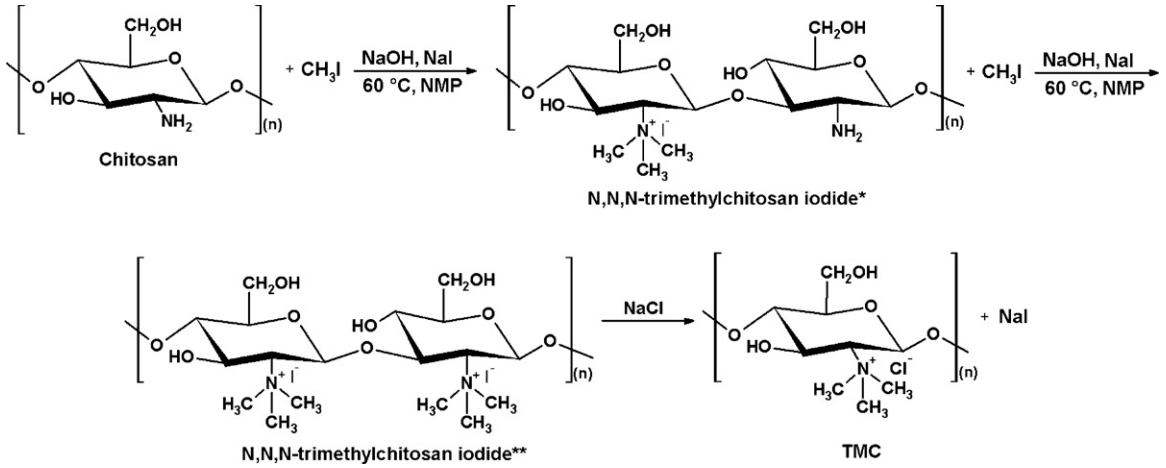

Fig. 1. Scheme of TMC synthesizes (*product from first step; **product from second step).

the TMC spectrum, which was assigned to the angular deformation of N–H bonds on CHT. Thus, from this observation the occurrence of the entirely *N*-methylation [$-NH_2 + 3(CH_3I) \rightarrow -N^+(CH_3)_3I^- + 2$ HI] reaction (Britto, Forato, & Assis, 2008; Mi et al., 2008) is expected. But, the band at 1555 cm^{-1} on TMC spectrum assigned to the N–H bending demonstrated that although the methylation of amino groups on CHT have been effectively occurred, the reaction was partial. Thus, the occurrence of substitution of one or both hydrogen atoms on amino groups of CHT generating, respectively, mono and disubstituted amino group would be possible. Furthermore, it can be observed in the TMC spectrum a shifting of bands at 2870–2920 cm^{-1} range assigned to axial deformation (symmetric and asymmetric) of C–H bonds, due to presence of methyl carbons on TMC structure. The higher amount of C–H bonds on TMC structure causes enhancement of such bands on TMC spectrum shifting them to higher wavenumber, as compared to the CHT spectrum (Mi et al., 2008). The characteristic band assigned to the vibrational stretching of –N–H bonds (3500–3600 cm^{-1}) is overlapped by the band assigned O–H (3000–3700 cm^{-1}) on CHT spectrum. The bands in the range of 2800–3600 cm^{-1} appear on TMC spectrum at higher wavenumber and are lesser intense than those of the CHT spectrum. This might be explained by reducing the amount of $-NH_2$ on TMC chains as compared to CHT. The bands assigned to –O–H and –N–H bonds only slightly overlap in TMC spectrum and a shoulder can be observed at ~3300 cm^{-1}. This information is significant to clarify the effectiveness of TMC synthesis.

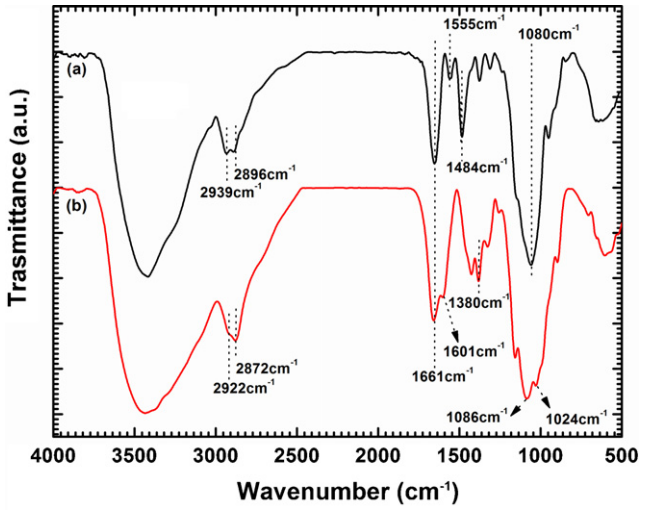

Fig. 2. FTIR spectra of TMC (a) and CHT (b).

The synthesis of TMC was also characterized through ^1H and CP-MAS ^{13}C NMR techniques. Analysis of CP/MAS ^{13}C NMR spectrum was used for examination of TMC structure and ^1H NMR spectrum of TMC was used for determination the degree of quaternization (DQ) of TMC. The data of such characterization are presented elsewhere (Martins et al., 2011). Briefly, the value of DQ of TMC, equal to 59%, was obtained through TMC ^1H NMR spectrum calculating the areas of the resonance signals assigned to hydrogen from acetamide groups (reference) and hydrogen assigned to *N*-dimethyl and *N*-trimethyl groups (due to the methylation reaction).

3.2. Characterization of PECs

The PECs prepared at pHs 5, 8, 10 and 12 were characterized through FTIR, DSC/TGA curves and WAXS. The analyses were made taking into account the differences existing in the data collected from different PEC samples and by comparison with data from precursors (TMC and HP). In all PECs preparation, the mass ratio of TMC to HP was kept constant: 0.1 g of TMC to 0.03 g of HP (Martins et al., 2011). As can be seen in the following discussion, the pH-conditions in which the PEC was prepared influenced the interactions between TMC and HP. Some evidences show that the pH-conditions may have been also influenced the complexation for obtaining PECs with effective TMC/HP ratio different from that used in the feed solution.

3.2.1. Characterization of PECs through FTIR

FTIR spectra of HP and TMC and of PECs prepared at pHs 5, 8, 10 and 12 are shown in Fig. 3. The characteristic bands that appear on the FTIR spectra of precursors (TMC and HP) are observed on FTIR spectra of PECs. Besides, it was observed that the band at 1555 cm^{-1} assigned to N–H bending of mono and disubstituted amino groups on TMC appears only slightly in the spectrum of PEC5. This shows that these groups are effectively complexed with HP mainly in PECs obtained on alkaline conditions. The bands that appear in the range from 1400 to 1650 cm^{-1} on FTIR spectrum of HP are due to the symmetric and asymmetric axial deformation of carboxylic groups (Ho, Mi, Sung, & Kuo, 2009).

These bands undergo significant changes due to complexation of the carboxylic groups ($-COO^-$) of HP with the quaternary nitrogen atoms of TMC, which are positively charged [$-N^+(CH_3)_3$]. The intensity of the band at 1429 cm^{-1} decreases in the FTIR spectra of PECs related to this same band on FTIR spectrum of HP.

The FTIR spectrum of HP exhibits bands that are assigned to axial deformation of S=O bonds, at 1239 cm^{-1}, and to axial deformation

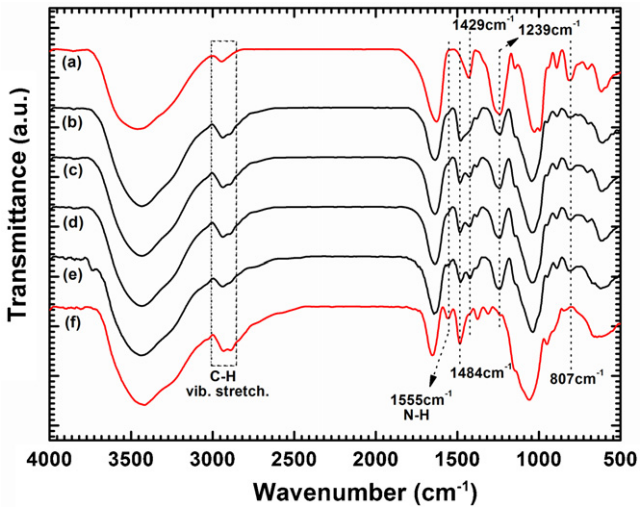

Fig. 3. FTIR spectra of pure HP (a), PEC12 (b), PEC10 (c), PEC8 (d), PEC5 (e) and TMC (f).

of C–O–S bonds from sulfonate groups, at 807 cm^{-1} (Grant, Long, & Williamson, 1987; Ho et al., 2009). In the FTIR spectra of PECs these bands can also be observed, however, with lesser intensity as compared to FTIR spectrum of raw HP. So, the electrostatic interactions among the positively charged [$-N^{+}(CH_3)_3$] groups on TMC and the carboxylic ($-COO^{-}$) and sulfonate ($-OSO_3^{-}$) groups on HP may be the responsible for such reduction in intensity. It is important to notice that the observed changes in the FTIR spectra of PECs related to precursors (HP and TMC) are dependent on the pH of feed solution at which the PEC was formed. The changes in the band-intensity and band shifting, due to electrostatic interactions among charged functional groups of TMC and HP, are different when the pH-condition, at which the complexation occurred, is taken into account. For instance, the decreasing in the intensities of the bands at 1484, 1429 and 1239 cm^{-1} is a pH-dependent behavior. The changes in interaction strength lead to materials with different and interesting properties.

3.2.2. Characterization of PECs through DSC/TGA curves

The TGA curves of different PECs and precursors (CHT, TMC and HP) are shown in Fig. 4a. Two stages of mass loss are observed in the TGA curves of HP, CHT, and TMC. The first one, at range from 25 to 125 °C, was attributed to the evaporation of water. It should be important to notice that those samples showed different content of water. HP presented the highest water content, CHT an intermediate quantity, while TMC showed the smallest value. HP presents in its structure groups such as carboxylate ($-COO^{-}$) and sulfonate ($-OSO_3^{-}$), which are highly hydrophilic and could strongly interact with water molecules through dipole–dipole or ion–dipole forces. For its side, CHT presents hydroxyl (–OH) and amino ($-NH_2$) groups that could provide some dipole-dipole interactions to water. The main reason for TMC presenting lesser water content than CHT is due to its high degree of quaternization (DQ). The incorporation of positive charges on nitrogen atoms of TMC should allow stronger interaction among water and TMC, compared to CHT. Britto and Campana-Filho (2004) published a work in which the TMC presented low DQ (5, 21 and 33%) being slightly more hydrophilic than the precursor (CHT), fact that was attributed to the quaternization of the nitrogen atoms of CHT. However, the TMC used for obtaining the PECs in this work possesses DQ equal to 59% (Martins et al., 2011) and the data collected from TGA curves showed a decrease on hydrophilicity of TMC, related to CHT. This was due to the concomitant methylation on C_3–OH and C_6–OH groups of CHT, fact confirmed through NMR analysis (Martins et al., 2011). Therefore, the high density of methyl groups at C_3–OCH_3, C_6–OCH_3 and the high DQ are the responsible for the higher hydrophobicity of TMC compared to CHT. The values of water content on precursors (CHT, TMC, and HP) and on PEC samples are given in Table 1.

Table 1
Temperatures for the first and second thermal events CHT, HP, TMC and PECs, from the TGA curves.

Sample	Temperature (°C)		Weight loss (%)
	Range	Peak (DTG)	
First event			
HP	25–125	–	17.5
CHT	25–125	–	9.2
TMC	25–125	–	3.9
PEC5	25–125	–	8.1
PEC8	25–125	–	14.4
PEC10	25–125	–	14.3
PEC12	25–125	–	12.3
Second event			
HP	200–269	269	47.5
CHT	200–312	312	59.8
TMC	200–264	264	52.9
PEC5	200–285	258	42.2
PEC8	200–288	268	35.4
PEC10	200–297	277	34.0
PEC12	200–348	285	35.7

The degradation of CHT, HP and TMC occurs on second stage of weight loss and are clearly showed in TGA curves of Fig. 4a. The exact value of temperature in which the second thermal event occurs for a given PEC sample is also presented in Table 1 and it was obtained through first derivative (DTG) of respective TGA curve, being the DTG curves shown elsewhere (Martins et al., 2011). It could be verified that CHT is more thermally stable than TMC (Britto & Campana-Filho, 2004) and HP. The smaller thermal stability of TMC related to CHT was ascribed to its high DQ (59%). In other words, it was due to the huge amount of methyl groups bonded on the nitrogen atoms and on C_3–OH and C_6–OH ones. The insertion of such methyl groups decreases the strength of intra-chain interactions, especially those from H-bonds (Britto & Campana-Filho, 2004).

As occurs in the TGA curves of CHT, HP and TMC, the TGA curves of PECs show two stages of weight loss, being the first stage attributed to loss of absorbed water and the second to the degradation. The content of water in PEC samples ranges from 8 up to 14%. Certainly, such values are dependent on the hydrophilicity of both polymers that constitute the PEC. In addition, the weight loss corresponding to the volatilization of water in the PECs is also dependent to pH-condition used for preparing the PEC. The charge density on HP at alkaline conditions (pH 8 or higher) is substantially elevated, compared to pH 5 one. At pH 5 the carboxylate groups on HP are partially ionized due to the p*Ka* of such groups be closer to 5 (Piai, Rubira, & Muniz, 2009). At pH ≤5 the TMC presents high density of positive charges due to its elevated DQ and due to possible protonation of the nitrogen atoms at mono and disubstituted sites ($^{+}NRH_2$ and $^{+}NR_2H$, being R = $-CH_3$). At alkaline conditions, the positive charges on TMC are derived mostly from the quaternized nitrogen atoms. Also, as the DQ of TMC is 59%, it could be asserted that the density of positive charges on TMC at alkaline conditions would be elevated. At pH 5 the density of positive charges on TMC is still high but, at the same time, such pH-condition favors only a low density of negative charges on HP. Therefore, at pH 5 the complexation of both polymers was not so effective and it is expected that the PEC5 being constituted of lower amount of HP in relation to feed solution.

PEC8 and PEC10 showed similar values of water content. At alkaline conditions both HP and TMC are highly ionizated, and then the complexation between these opposite charged polymers occurs

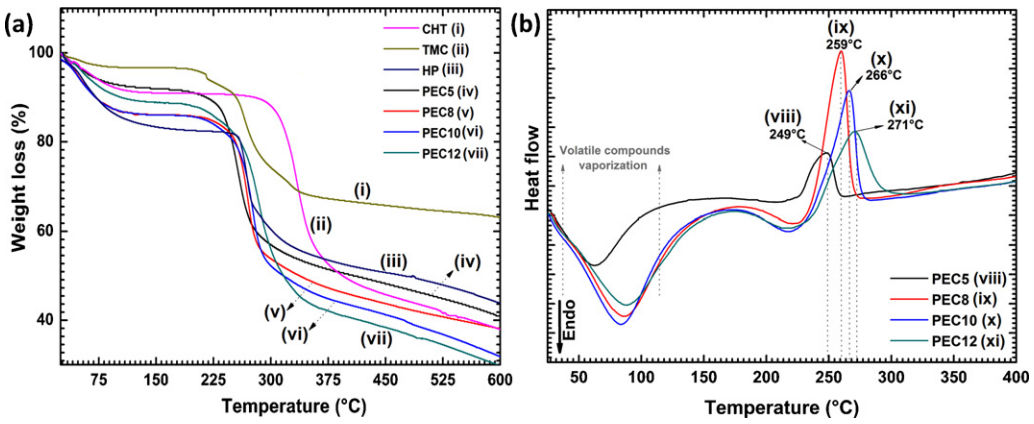

Fig. 4. (a) TGA curves of TMC/HP complexes formed at different pH conditions and raw materials CHT, TMC and HP. (b) DSC curves of TMC/HP complexes formed at different pH conditions.

more effectively than at acidic conditions (pH 5). It was verified higher HP content on PEC8 and PEC10 related to PEC5. Considering that HP is more hydrophilic than TMC, the higher water contents on PEC8 and PEC10 related to PEC5 were attributed to the contents of HP in PEC8 and PEC12 to be close to used on the feed. Besides, the existence of intermolecular interactions among the water molecules and the nitrogen atoms on mono and disubstituted neutral sites of TMC might also have contributed to raising the amount of water in PEC8 and PEC10.

The density of positive charges of TMC at pH 12 is high and practically the same that at pHs 8 and 10 due to the fact that those charges arise from the same amount of quaternized nitrogen atoms. In addition, at pH >7, the functional groups from HP chains are negatively charged and then they interact strongly by electrostatic interactions with the positively charged groups from TMC.

The strongest interactions on PEC12 should be the responsible for the decreasing in the water content in this PEC related to PEC8 and PEC10. In PEC12 the polymer chains are closer and the strength of interactions among opposite electrical charges is much higher than those among ion–dipole interactions (water/HP or water/TMC).

The DSC curves of PECs are shown in Fig. 4b. The endothermic peaks that appear in the range of 25 to c.a. 125 °C of DSC curves of PECs were attributed to the vaporization of adsorbed and bounded water and match to the TGA curves. The exothermic peaks in the range from ca. 220 to 300 °C are related to the thermal degradation of PECs. The DSC curves also corroborate to the TGA curves, which show the increasing stability of polyelectrolyte complexes as the pH of feed solution, used for PEC preparing, is increased. It was suggested that the increasing on pH-condition contributed to form more stable complexes due to the growing on strength of interactions between TMC and HP. Comparing the values of degradation temperature (collected from DTG curves) at the two extremes pH-condition used in this work, PEC5 and PEC12, a difference of ca. 27 °C was observed. The PEC5 presented lower degradation temperature (peak from DTG) as compared to TMC one.

Fig. 5 shows the dependence of the degradation temperatures of PECs, collected from the TGA and DSC curves, against the pH of the feed solution. According to the plot, the thermal stability increases linearly with the increase of pH, for both TGA and DSC data, according to following equations:

$$T_{D1} = 239.2 + 3.8\,\mathrm{pH}\,(\text{from TGA data};\ R^2 = 0.997) \quad (1)$$

$$T_{D2} = 233.4 + 3.2\,\mathrm{pH}\,(\text{from DSC data};\ R^2 = 0.994) \quad (2)$$

where T_{D1} and T_{D2} are the temperatures of degradation (T_{D1} were obtained from the TGA curves; and T_{D2} were obtained from the maximum of exothermic peaks from DSC curves); and pH is the pH-condition in which each PEC sample was formed.

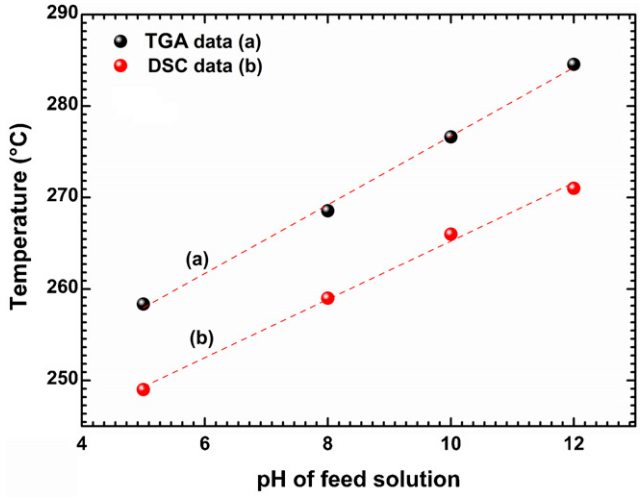

Fig. 5. Dependence of degradation temperature to pH of TMC feed solution calculated from (a) DTG and (b) maximum of exothermic peaks from DSC curves.

3.2.3. *Characterization of PECs through WAXS profiles*

Fig. 6 shows the WAXS profiles of CHT, TMC and HP, and of PEC5, PEC8, PEC10, and PEC12. The WAXS profile of HP exhibited a broad diffraction peak with low intensity in the range (2θ) from 15° to 30° that characterizes its low crystallinity. CHT WAXS profile exhib-

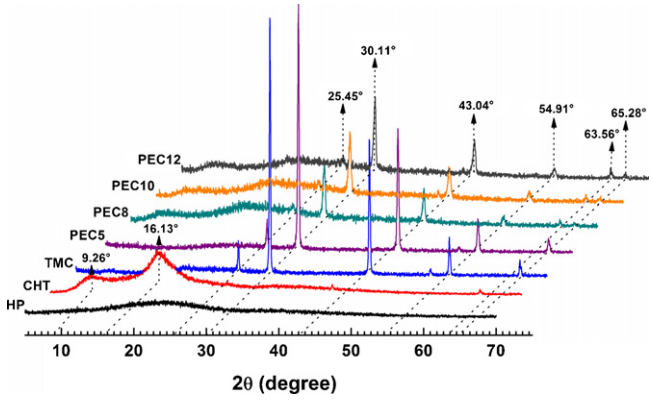

Fig. 6. WAXS profiles of pure HP and CHT, TMC and PEC samples.

Table 2
Areas of diffraction peaks at $2\theta = 30.11^\circ$ (P1), 43.04° (P2) and 54.91° (P3) observed on PECS and TMC WAXS profile (diffractogram shown in Fig. 6).

	Diffraction peak areas (a.u.)		
	P1 ($2\theta = 30.11^\circ$)	P2 ($2\theta = 43.04^\circ$)	P3 ($2\theta = 54.91^\circ$)
TMC	0.252	0.150	0.054
PEC5	0.292	0.165	0.058
PEC8	0.710	0.354	0.152
PEC10	0.688	0.344	0.132
PEC12	0.638	0.304	0.122

ited two broad diffraction peaks at $2\theta = 9.26^\circ$ and 16.13° which confirm presence of crystalline domains on CHT structure. These crystalline domains are attributed to ordered regions formed by hydrogen bonds among the amino groups on CHT chains (Fajardo, Piai, Rubira, & Muniz, 2008; Piai et al., 2009).

Significant differences between the WAXS profiles of CHT and TMC can be observed. WAXS profile of TMC exhibits well-defined diffraction peaks because the salt form of TMC (see Fig. 1) that easily crystallizes. Intense diffraction peaks at $2\theta = 25.45^\circ$, 30.11°, 43.04°, 54.91°, 63.56° and 65.28° are present in WAXS profile of TMC suggesting the formation of crystalline regions with different periodic distances. On the other hand, the diffraction peaks exhibited by raw CHT are no longer present in the TMC WAXS profile. This happened because the methylation process on CHT disrupts the hydrogen bonds among the amino groups (Britto & Campana-Filho, 2004).

The charge formation on amino groups [$-N^+(CH_3)$] promotes rising on cation–cation repulsion and consequent destabilization of ordered regions, commonly observed in WAXS profile of CHT. At pH 5, the interactions between chloride ions and [$-N^+(CH_3)$] groups of TMC are so strong that hinders the interaction to partially ionized HP, so disfavoring the complexation. For this reason, the WAXS profiles of PEC5 and TMC are wholly similar. Concerning to the other PECs (PEC8, PEC10 and PEC12), some differences in diffraction peaks intensities could be observed on WAXS profiles of such PECs related to TMC WAXS profile. The electrostatic interactions existing on PECs prepared at alkaline conditions disturb the interactions among chloride ions and nitrogen charged ions ($^+NRH_2$, $^+NR_2H$ and $^+NR_3$, being R = $-CH_3$) and led a decreasing the crystallinity as compared to that existing on not complexed TMC. A small diffraction peak at $2\theta = 63.56^\circ$ was observed on WAXS profiles of PEC8, PEC10 and PEC12 but not present on WAXS profiles of TMC and PEC5. The intensity of this peak clearly increases as the pH changes from 8 to 12. In addition, the intensity of peak at $2\theta = 63.28^\circ$, strong on WAXS profiles of TCM and PEC5, is weakened on WAXS profiles of PEC8, PEC10 and PEC 12. These facts were attributed to the smaller distance between TMC and HP chains on PECs prepared at pH $\geq$8. The formation of new ordered regions on these complexes could be associated to increase of thermal stability on PECs prepared at alkaline conditions, compared to PEC5 and to TMC.

The changes on intensities of diffraction peaks at $2\theta = 30.11^\circ$ (P1), 43.04° (P2) and 54.91° (P3) on WAXS profiles of PECs were evaluated through the ratio in area of these diffraction peaks to the area of respective diffraction peaks on WAXS profile of TMC. The results are shown in Table 2.

4. Conclusions

N,*N*,*N*-trimethyl chitosan (TMC) was synthesized through the *N*-methylation of chitosan (CHT) and characterized by FTIR spectroscopy. PECs based on TMC and heparin (HP) were prepared at different pH-conditions. The solubility of TMC at a wide range of pH allowed preparing such PECs that were characterized through FTIR, TGA, DSC, and WAXS. The pH of feed solution used for preparing the PEC strongly influences some PEC properties. FTIR data show that the PEC prepared at pH 5 presented small complexation effectiveness as compared to the PECs prepared at alkaline conditions. This fact was attributed to high density of positive charges and high degree of quaternization (DQ = 59%) of TMC. From DSC and TGA curves, it was verified that the thermal stability of PECs is higher as higher is the pH of feed solution used for PEC forming. At alkaline medium (pH >7), the complexation of TMC and HP is more effective, because the functional groups from HP are completely ionized under these conditions. WAXS profiles of PECs show alterations related to WAXS of TMC and show that the PEC crystallinity depends on the pH used for complexation. These results match to the FTIR, TGA, and DSC data. Due to stronger electrostatic interactions at higher pHs the unlike polymers chains (TMC and HP) are closer enough to produce more stable PECs.

Acknowledgements

A.F.M. thanks to Fundação Araucária (Paraná, Brazil) by master's fellowship. A.G.B.P. and A.R.F. thanks to Capes (Brazil) by doctorate's fellowships. A.F.R. and E.C.M. thanks to CNPq by financial support (Proc. 481424/2010-5).

References

Abdel-Fattah, W. I., Jiang, T., El-Bassyouni, G. E. T., & Laurencin, C. T. (2007). Synthesis, characterization of chitosans and fabrication of sintered chitosan microsphere matrices for bone tissue engineering. *Acta Biomaterialia*, *3*, 503–514.

Britto, D., & Campana-Filho, P. S. (2004). A kinetic study on the thermal degradation of *N*,*N*,*N*-trimethylchitosan. *Polymer Degradation and Stability*, *84*, 353–361.

Britto, D., Forato, A. L., & Assis, O. B. G. (2008). Determination of the average degree of quaternization of *N*,*N*,*N*-trimethylchitosan by solid-state ^{13}C NMR. *Carbohydrate Polymers*, *74*, 86–91.

Chang, Y. H., Xiao, L., & Du, Y. M. (2009). Preparation and properties of a novel thermosensitive N-trimethyl chitosan hydrogel. *Polymer Bulletin*, *63*, 531–545.

Chen, F., Zhang, Z.-R., Yuan, F., Qin, X., Wang, M., & Huang, Y. (2008). In vitro and in vivo study of N-trimethyl chitosan nanoparticles for oral protein delivery. *International Journal of Pharmaceutics*, *349*, 226–233.

Chen, Z., Mo, X., He, C., & Wang, H. (2008). Intermolecular interactions in electrospun collagen–chitosan complex nanofibers. *Carbohydrate Polymers*, *72*, 410–418.

Fajardo, A. R., Piai, J. F., Rubira, A. F., & Muniz, E. C. (2008). Time- and pH-dependent self-rearrangement of a swollen polymer network based on polyelectrolytes complexes of chitosan/chondroitin sulfate. *Carbohydrate Polymers*, *80*, 934–943.

Fu, J., Ji, J., Yuan, W., & Shen, J. (2005). Construction of anti-adhesive and antibacterial multilayer films via layer-by-layer assembly of heparin and chitosan. *Biomaterials*, *26*, 6684–6692.

George, M., & Abraham, T. E. (2006). Polyionic hydrocolloids for the intestinal delivery of protein drugs: Alginate and chitosan – a review. *Journal of Controlled Release*, *114*, 1–14.

Grant, D., Long, W. F., & Williamson, F. B. (1987). Infrared spectroscopy of heparin cation complexes. *Biochemical Journal*, *244*, 143–149.

Hamman, J. H., & Kotzé, A. F. (2001). Effect of the type of base and number of reaction steps on the degree of quaternization and molecular weight of N-trimethyl chitosan chloride. *Drug Development and Industrial Pharmacy*, *27*, 373–380.

Ho, Y. C., Mi, F. L., Sung, H. W., & Kuo, P. L. (2009). Heparin-functionalized chitosan–alginate scaffolds for controlled release of growth factor. *International Journal of Pharmaceutics*, *376*, 69–75.

Jintapattanakit, A., Junyaprasert, V. B., Mao, S., Sitterberg, J., Bakowsky, U., & Kissel, T. (2007). Peroral delivery of insulin using chitosan derivatives: A comparative study of polyelectrolyte nanocomplexes and nanoparticles. *International Journal of Pharmaceutics*, *342*, 240–249.

Kotzé, A. F., Luessen, H. L., De Leeuw, B. J., De Boer, B. G., Verhoef, J. C., & Junginger, H. E. (1997). N-trimethyl chitosan chloride as a potential absorption enhancer across mucosal surfaces: In vitro evaluation in intestinal epithelial cells (Caco-2). *Pharmaceutical Research*, *14*, 1197–1202.

Kweon, D.-K., Song, S.-B., & Park, Y.-Y. (2003). Preparation of water-soluble chitosan/heparin complex and its application as wound healing accelerator. *Biomaterials*, *24*, 1595–1601.

Le Dung, P., Milas, M., Rinaudo, M., & Desbriires, J. (1994). Water soluble derivatives obtained by controlled chemical modifications of chitosan. *Carbohydrate Polymers*, *24*, 209–214.

Li, X. Y., Li, X., Kong, X. Y., Shi, S., Guo, G., Zhang, J., Luo, F., Zhao, X., Wei, Y. Q., Qian, Z. Y., & Yang, L. (2010). Preparation of N-trimethyl chitosan–protein nanoparticles intended for vaccine delivery. *Journal of Nanoscience and Nanotechnology*, *10*, 4850–4858.

Lin, Y. H., Chang, C. H., Wu, Y. S., Hsu, Y. M., Chiou, S. F., & Chen, Y. J. (2009). Development of pH-responsive chitosan/heparin nanoparticles for stomach-specific anti-*Helicobacter pylori* therapy. *Biomaterials*, *30*, 3332–3342.

Liu, Y.-L., Jiang, S., Ke, Z.-M., Wu, H.-S., Chi, C.-H., & Guo, Z.-Y. (2009). Recombinant expression of a chitosanase and application in chitosan oligosaccharide production. *Carbohydrate Research*, *344*, 815–819.

Martins A. F., Piai J. F., Schüquel I. T. A., Rubira A. F., & Muniz E. C. (2011) Polyelectrolyte complexes of chitosan/heparin and *N*,*N*,*N*-trimethylchitosan/heparin obtained at different pHs: I. Preparation, characterization and essays of controlled release of heparin. *Journal of Colloid and Polymer Science*, 289, 1133-1144.

Mi, F.-L., Sung, H.-W., Shyu, S.-S., Su, C.-C., & Peng, C.-K. (2003). Synthesis and characterization of biodegradable TPP/genipin co-crosslinked chitosan gel beads. *Polymer*, *44*, 6521–6530.

Mi, F.-L., Wu, Y.-Y., Lin, Y.-H., Sonaje, K., Ho, Y.-C., Chen, C.-T., Juang, J.-H., & Sung, H.-W. (2008). Oral delivery of peptide drugs using nanoparticles self-assembled by poly(γ-glutamic acid) and a chitosan derivative functionalized by trimethylation. *Bioconjugate Chemistry*, *19*, 1248–1255.

Mourya, V. K., & Inamdar, N. N. (2009). Trimethyl chitosan and its applications in drug delivery. *Journal of Materials Science – Materials in Medicine*, *20*, 1057–1079.

Oyarzun-Ampuero, F. A., Brea, J., Loza, M. I., Torres, D., & Alonso, M. J. (2009). Chitosan–hyaluronic acid nanoparticles loaded with heparin for the treatment of asthma. *International Journal Pharmaceutics*, *381*, 122–129.

Piai, J. F., Lopes, L. C., Fajardo, A. R., Rubira, A. F., & Muniz, E. C. (2010). Kinetic study of chondroitin sulphate release from chondroitin sulphate/chitosan complex hydrogel. *Journal of Molecular Liquids*, *156*, 28–32.

Piai, J. F., Rubira, A. F., & Muniz, E. C. (2009). Self-assembly of a swollen chitosan/chondroitin sulfate hydrogel by outward diffusion of the chondroitin sulfate chains. *Acta Biomaterialia*, *5*, 2601–2609.

Polnok, A., Borchard, G., Verhoef, J. C., Sarisuta, N., & Junginger, H. E. (2004). Influence of methylation process on the degree of quaternization of N-trimethyl chitosan chloride. *European Journal of Pharmaceutics and Biopharmaceutics*, *57*, 77–83.

Sadeghi, A. M. M., Dorkoosh, F. A., Avadi, M. R., Saadat, P., Rafiee-Tehrani, M., & Junginger, H. E. (2008). Preparation, characterization and antibacterial activities of chitosan, N-trimethyl chitosan (TMC) and N-diethylmethyl chitosan (DEMC) nanoparticles loaded with insulin using both the ionotropic gelation and polyelectrolyte complexation methods. *International Journal of Pharmaceutics*, *355*, 299–306.

Sayin, B., Somavarapu, S., Li, X. W., Thanou, M., Sesardic, D., Alpar, H. O., & Senel, S. (2008). Mono-N-carboxymethyl chitosan (MCC) and N-trimethyl chitosan (TMC) nanoparticles for non-invasive vaccine delivery. *International Journal of Pharmaceutics*, *363*, 139–148.

Sieval, A. B., Thanou, M. M., Kotzé, A. F., Verhoef, J. C., Brussee, J., & Junginger, H. E. (1998). Preparation and NMR characterization of highly substituted N-trimethyl chitosan chloride. *Carbohydrate Polymers*, *36*, 157–165.

Snyman, D., Hamman, J. H., Kotze, J. S., Rollings, J. E., & Kotzé, A. F. (2002). The relationship between the absolute molecular weight and the degree of quaternization of N-trimethyl chitosan chloride. *Carbohydrate Polymers*, *50*, 145–150.

Thanou, M., Florea, B. I., Langemeyer, M. W., Verhoef, J. C., & Junginger, H. E. (2000). N-trimethylated chitosan chloride (TMC) improves the intestinal permeation of the peptide drug buserelin in vitro (Caco-2 cells) and in vivo (rats). *Pharmaceutical Research*, *17*, 27–31.

Thanou, M., Verhoef, J. C., & Junginger, H. E. (2001). Oral drug absorption enhancement by chitosan and its derivatives. *Advanced Drug Delivery Reviews*, *52*, 117–126.

Thanou, M., Verhoef, J. C., Marbach, P., & Junginger, H. E. (2000). Intestinal absorption of octreotide: N-trimethyl chitosan chloride (TMC) ameliorates the permeability and absorption properties of the somatostatin analogue in vitro and in vivo. *Journal of Pharmaceutical Sciences*, *89*, 951–957.

Van der Merwe, S. M., Verhoef, J. C., & Verheijden, J. H. M. (2007). Enhancer for improved per oral delivery of peptide drugs. *European Journal of Pharmaceutics and Biopharmaceutics*, *58*, 225–235.

Xu, T., Xin, M., Li, Mingchun, Huang, H., & Zhou, S. (2010). Synthesis, characteristic and antibacterial activity of *N*,*N*,*N*-trimethyl chitosan and its carboxymethyl derivates. *Carbohydrate Polymers*, *81*, 931–936.

Yuan, Q., Hein, S., & Misra, R. D. K. (2010). New generation of chitosan-encapsulated ZnO quantum dots loaded with drug: Synthesis, characterization and in vitro drug delivery response. *Acta Biomaterialia*, *6*, 2732–2739.

Yuan, Y., Chesnutt, B. M., Utturkar, G., Haggard, W. O., Yang, Y., Ong, J. L., & Bumgardner, J. D. (2007). The effect of cross-linking of chitosan microspheres with genipin on protein release. *Carbohydrate Polymers*, *68*, 561–567.

Zhu, A. P., Ming, Z., & Jian, S. (2005). Blood compatibility of chitosan/heparin complex surface modified e PTFE vascular graft. *Applied Surface Science*, *241*, 485–492.